JOURNAL OF OPTOELECTRONICS AND ADVANCED MATERIALS, Vol. 9, No. 10, October 2007, p. 3278 - 3284

Structural and atomic transport properties of molten zinc oxide

S. SENTURK DALGIC*, O. OZGEC
Department of Physics, Trakya University, 22030, Edirne, Turkey

We present a theoretical study of the static structure and atomic transport properties of molten Zinc Oxide using different effective pair potentials. Semi-empirical potentials such as a three body potential of Tersoff and Kohen-Tully-Stillinger have been applied. The pair correlation functions for ZnO above melting point has predicted by Variational Hypernetted Chain Liquid State theory (VMHNC). The dynamics and atomic transport properties of ZnO have been studied with the viscoelastic model approximation by computing both single-particle and collective time-dependent properties. The mean –square displacement, the velocity autocorrelation function and the intermediate scattering function have obtained inorder to compute the self diffusion coefficients at different temperatures. For comparison, the calculations are also performed using the rigid ion model potentials. It is shown that the calculated liquid structural properties predicted by Tersoff potential are in good agreement with the latest theoretical results.

(Received July 3, 2007; accepted October 1, 2007)

Keywords: Semi–empirical potentials, Structure, Molten Zinc Oxide

1. Introduction

Zinc oxide is an interesting material with a range of technological applications including electronic and electro-optic devices, catalysis, chemical sensors, and conductive solar cell window layers. In recent years, ZnO has received a particular attention as a semiconductor which also has a close affinity with ionic insulators such as MgO. ZnO can be transformed to the characteristically ionic rocksalt structure by relatively modest hydrostatic pressures, and unlike most semiconductors this cubic high-pressure phase remains metastable even at zero pressure [1]. Also, its high-pressure and high-temperature behaviors have long been a subject of great interest for experimental and theoretical investigations [1-15]. Experimentalists have been studied with bulk properties of ZnO such as lattice constant [2], equilibrium volume [3] and elastic constants [4]. In addition to these, the experimental studies are generally interested in structural phase transition in ZnO [3, 5-6].

Among the theoretical studies on ZnO, Jaffe and co-workers used local-density and generalized gradient approximations (LDA and GGA) to calculate high-pressure phase transitions in ZnO and MgO and also reported total energy and electronic structure calculations of ZnO [7]. Furthermore Sun and co-workers were investigated structural, electronic and dynamic properties of ZnO with the pair-wise potential of the Buckingham form using the molecular dynamics (MD) method [8-12]. Zaoui and Sekkal studied with the high pressure effect on the structural transition in ZnO using the Buckingham potential [13]. Aoumeur and co-workers have calculated the structural and dynamical properties of ZnO in zinc blend and rocksalt phases [1]. They have used the molecular dynamics simulation based on Tersoff Potential (TP) [14] in order to calculate the equilibrium lattice parameters, bulk modulus, pressure derivatives, the elastic constants, and the thermal properties [1]. However they have not reported the validity of TP potential model in the dynamics calculation of ZnO near its melting.

Another point of view on the semi-empirical potential model of Tersoff, Benkabou and co-workers has been interested in testing the transferability of a three-body Tersoff potential for SrO [15]. They have concluded that an empirical three body TP potential with MD method reproduces well the structural properties of alkaline earth oxides in their different high pressure phases. In a recent series of our previous work, we have successfully applied the Tersoff potential to obtain the structural properties of CuI [16], CuBr, CuCl [17] and BaO [18] using the integral equation theories. These studies are motivated us to apply the Tersoff potential for ZnO.

In this paper we present the structural, dynamical and thermal properties of ZnO in the liquid structure, using the empirical interatomic potentials of Tersoff (TP), Kohen-Tully-Stillinger (KTS) [19] and Buckingham (BP) potentials [12]. According to our knowledge, no structural calculations have been performed on molten ZnO using these potentials coupled with integral equations. The main point of the present work is the test of the transferability of semi-empirical potential models to predict structural properties of molten ZnO coupled with integral equations. For this purpose, first we have calculated the inter-ionic interactions in ZnO using TP, KTS and BP potentials model which is used as input data in its structural calculations with the variational modified hypernetted chain (VMHNC) integral equation theory. Then, those potential accuracies have been tested in the structural calculations for ZnO at different temperatures. The computed pair distribution functions of ZnO have been compared with each other and those obtained by MD results of Sun [8]. The second aim in this work is also

compute the dynamic properties of molten ZnO near its melting. The atomic transport properties evaluated within the framework of modecoupling theory, using a self-consistent scheme have been also presented. The single-particle dynamics of the system has been analyzed by computing the mean square displacement (MSD) and velocity autocorrelation function (VACF). Temperature dependence of self diffusion coefficient has also been shown. The collective dynamic properties such as the intermediate scattering function have determined. We have shown that Tersoff potential can be applied to ZnO successfully.

2. Theory

2.1 Semi empirical potentials:

2.1.1 Tersoff Potential

Among the many empirical model potentials that have been developed for tetrahedral semiconductors, that of Tersoff has been applied to many of the semiconductors successfully. The interatomic potential is taken to have the form as [14]

$$E = \sum_i E_i = \frac{1}{2}\sum_{i \neq j} V_{ij} \quad , \tag{1}$$

$$V_{TP} = f_C(r_{ij})[a_{ij}\ f_R(r_{ij}) + b_{ij}\ f_A(r_{ij})], \tag{2}$$

where E is the total energy of the system, which is decomposed for convenience into a site energy E_i and band energy V_{ij}. The indices i and j ion over the atoms of the system and r_{ij} is the distance from atom i to atom j. The function f_R represents a repulsive potential and f_A represents an attractive pair potential associated with bonding given as

$$f_R(r) = A\exp(-\lambda_1 r)\,, \tag{3}$$

$$f_A(r) = -B\exp(-\lambda_2 r)\,. \tag{4}$$

The term f_c is merely a smooth cut of function to limit the range of potential taken as,

$$f_C(r) = \begin{cases} 1 & r < R - D \\ \frac{1}{2} - \frac{1}{2}\sin\left[\frac{\pi}{2}\frac{(r-R)}{D}\right] & R - D < r < R + D \\ 0 & r > R + D \end{cases} \tag{5}$$

where b_{ij} is the many-body order parameter describing how the bond-formation energy is affected by local atomic arrangement due to the presence of other neighboring atoms (the k atoms). It is a many-body function of the positions of atoms i, j and k given as

$$b_{ij} = \left(1 + \beta^n \zeta_{ij}^n\right)^{-1/2n}, \tag{6}$$

$$\zeta_{ij} = \sum_{k(\neq i,j)} f_C(r_{ik})\, g(\theta_{ijk}) \exp[\lambda_3^3 (r_{ij} - r_{ik})^3] \tag{7}$$

$$g(\theta) = 1 + \frac{c^2}{d^2} - \frac{c^2}{d^2 + (h - \cos\theta)^2}\,, \tag{8}$$

$$a_{ij} = (1 + \alpha^n \eta_{ij}^n)^{-1/2n}, \tag{9}$$

$$\eta_{ij} = \sum_{k(\neq i,j)} f_C(r_{ik}) \exp[\lambda_3^3 (r_{ij} - r_{ik})^3], \tag{10}$$

where ζ is defined as the effective coordination number and $g(\theta)$ is a function of the angle between r_{ij} and r_{ik}. Following others [14-16], we assume that λ_3 and α are maintained to be zero, thus a_{ij}=1. Other adjustable fitting parameters, A, B, n, c, d, h, λ_1 and λ_2 are determined by fitting to the cohesive properties of the material.

2.1.2 Kohen-Tully-Stillinger Potential (KTS)

We have chosen to use the extended SW potential, namely KTS potential [19]. It has been tested successfully for its accuracy in describing the CuI system in recent studies [16, 17]. The KTS potential energy V is a sum of two and three body interactions given by,

$$V_{KTS} = \sum_{\substack{i,j \\ i<j}} V_2(i,j) + \sum_{\substack{i,j,k \\ i<j<k}} V_3(i,j,k), \tag{11}$$

where the two-body term given as

$$V_2(r_{ij}) = \begin{cases} \xi_{ij}(C_{ij} r_{ij}^{-p} - 1)\exp[\kappa_{ij}/(r_{ij} - \ell_{ij})], & r_{ij} < \ell_{ij} \\ 0, & r_{ij} \geq \ell_{ij} \end{cases} \tag{12}$$

and the three-body term as

$$V_3(r_{ij}, r_{jk}, r_{ki}) = H(r_{ij}, r_{ik}, \theta_{jik}) + H(r_{jk}, r_{ji}, \theta_{ijk}) + H(r_{ki}, r_{kj}, \theta_{jki}) \tag{13}$$

Here H is taken as

$$H(r_{ij}, r_{ik}, \theta_{jik}) = \begin{cases} \varepsilon_{jik}(1 + \mu_{jik}\cos\theta_{jik} + \upsilon_{jik}\cos^2\theta_{jik})\exp[\Gamma(\gamma, r\chi)], \text{if } r_{ij} < \chi_{jik}, r_{ik} < \chi_{jik}, \\ 0, \text{ otherwise} \end{cases} \tag{14}$$

where $\Gamma(\gamma, r\chi)$,

$$\Gamma(\gamma, r, \chi) = \frac{\gamma_{ij(k)}}{r_{ij} - \chi_{jik}} + \frac{\gamma_{ik(j)}}{r_{ik} - \chi_{jik}}\ , \qquad (15)$$

where r is the distance between a pair of atoms, ℓ_{ij} and χ_{jik} are the cut-off distances of the two-body and the three-body potentials, respectively, and θ_{ijk} is the vertex angle at j subtended by i and k. $\xi_{ij}, C_{ij}, p,$ and κ_{ij} are fixed parameters chosen by fitting to the cohesive properties of the material. Parameters $\varepsilon_{jik}, \mu_{jik}, \upsilon_{jik}, \gamma_{ij(k)}$, and $\gamma_{ik(j)}$ are constants chosen to give best possible values for the structure.

2.2 Rigid Ion Potentials

2.2. 1. Buckingham Ionic Potential

The interatomic potential energy is the sum of the long-range Coulombic and short-range non-Coulombic contributions. For ionic materials the short-range interaction in the form of a Buckingham potential is a rather traditional model which has been shown to perform sufficiently well [20] and, therefore, widely used for modeling of various oxides. The advantages and shortcomings of these kinds of models are known from Ref. [21]. We use the Coulombic potential with a simple analytical expression of the Buckingham type for the short-range interaction between ions *i* and j:

$$V_{BP}(r_{ij}) = \frac{Z_i Z_j e^2}{r_{ij}} + A_0 \exp(-r_{ij}/B_0) - C_0 r_{ij}^{-6}, \qquad (16)$$

where the right-hand side terms represent repulsion energy and van der Waals force (dipole-dipole term), respectively. Here A_0 and B_0 are the parameters for the repulsive interaction, C_0 is van der Waals constant, r_{ij} is the interatomic distance between *i* and *j*.

2.3 Liquid State Theory

With the effective pair potential known, integral equations are able to provide us the liquid structure for metals and alloys. In our structural calculations, one of the integral equation theory which have shown very reliable theory of liquids VMHNC has been carried out [22-24]. Like most liquid state theories the VMHNC is solved the Ornstein – Zernike (OZ) equation by the MHNC exact closure relation. Thus, the partial direct correlation functions, $c_{ij}(r)$, in terms of the total correlation functions $h_{ij}(r)=g_{ij}(r)-1$, where $g_{ij}(r)$ denote the partial pair distribution, can be obtained. The pair distribution function can be given in terms of Ashcroft-Langreth partial structure factor as,

$$g_{ij}(r) = 1 + \frac{1}{8\pi^3(\rho_i \rho_j)^{1/2}} \int (S_{ij}(q) - \delta_{ij}) \exp(iqr) dq\,. \qquad (17)$$

2.4 Atomic Transport Properties

The transport properties (viscosity and diffusivity) are important for metallurgical process as well as for understanding the atomic dynamics of liquids. Generally two methods are available for computing the self diffusion coefficient D. The first one can be expressed by an Einstein expression, as related to the slope at large times of mean square displacement of tagged particle in the liquid,

$$D = \lim_{t\to\infty} \frac{\left\langle \Delta r(t)^2 \right\rangle}{6t}, \qquad (18)$$

where $< \Delta r(t)^2 >$ defined as the mean square displacement (MSD) of a tagged particle. The mean square displacement of atoms can be easily computed from its definition:

$$MSD = \{r(t) - r(0)\}^2. \qquad (19)$$

The second method relates to the velocity autocorrelation function Z(t) which was called Green-Kubo relation by [25-27],

$$D = \frac{k_B T}{m} \int_0^\infty Z(t) dt \qquad (20)$$

These two functions are related to each other by,

$$\Delta r^2(t) = \frac{6k_b T}{m} \int_0^t d\tau (t - \tau) Z(\tau) \qquad (21)$$

The central magnitude in the present analysis is the memory function of normalized velocity autocorrelation function, K(t), defined by the following Volterra-type equation

$$\dot{Z}(t) = -\int_0^t K(t - t') Z(t') dt' \qquad (22)$$

where the dot means time derivative of the normalized velocity autocorrelation function. The memory function may be split into two contributions [25],

$$K(t) = K_B(t) + K_{MC}(t) \qquad (23)$$

which represent two distinct dynamical regimes in the atomic dynamic of a liquid. The first term comprises all the fast decay channels. $K_B(t)$ is supposed to represent the effect of a binary collision between a targed particle and

another one from its environment whereas the second term, $K_{MC}(t)$ is the mode coupling contribution, incorporates the contribution from the collective processes associated with multiple collisions.

The inclusion of a slowly decaying time tail in memory function is known to be an essential ingredient for the correct description of the dynamics of a tagged particle in a fluid. In principle, coupling to several modes, should be considered such as density-density coupling, density longitudinal current coupling and density transversal current coupling but for the density/temperature range considered in this work the most important contribution arises from density-density coupling. Restricting the mode-coupling component to the density-density coupling term,

$$K_{MC}(t) = \frac{\rho k_B T}{24\pi^3 m}\int d\vec{q} q^2 c^2(q)\left[F_s(q,t)F(q,t) - F_0(q,t)F_B(q,t)\right] \quad (24)$$

Here c(q) denotes the direct correlation function of the liquid. F(q,t) and $F_s(q,t)$ are the intermediate scattering function and its self part, whereas $F_B(q,t)$, $F_0(q,t)$ denote the binary part of F(q,t) and $F_s(q,t)$ respectively. The intermediate scattering function F(q,t) [24-28] is given by

$$F(q,t) = F_B(q,t)\frac{F_s(q,t)}{F_0(q,t)}. \quad (25)$$

The temperature dependence of diffusion coefficient data exhibits the Arrhenius-type behavior:

$$D(T) = D_0 \exp(-E_a/RT) \quad (26)$$

where D_0 is the self diffusion prefactor, E_a is diffusional activation energy, R is the gas constant (*8.314 J/mol·K)* and T is absolute temperature in Kelvins.

3. Results and discussion

Firstly, we have presented pair interactions in ZnO using semi-empirical potentials such as Tersoff Potential (TP) and Kohen-Tully-Stillinger (KTS) potential. We separate KTS potential such as two and three body interactions KTS-V2 and KTS-V3 respectively and the KTS potential is the sum of these interactions. The all parameters of TP and KTS functions used in structural calculations are determined by fitting to cohesive energy which we used $E_c = -5.41eV$ [29] and taking into account for the cut-off procedure together with the VMHNC liquid state theory. The adjusted potential parameters for semi empirical potentials are presented in Table 1-2. The BP potential parameters are taken from Sun and co-workers [8].

Table 1. The adjusted TP parameters for ZnO.

A(eV)	4099.2	β	1.1×10^{-6}
B(eV)	200.0	c	100390
$\lambda_1(A^{-1})$	3.2599	d	16.217
$\lambda_2(A^{-1})$	1.7322	R(A)	6.255
n	0.7873	D(A)	0.65
h	-5.7058		

Table 2. The adjusted KTS potential parameters for ZnO.

ξ(eV)	69.352	ε(eV)	29.748
$C(A^p)$	12.798	μ	-5.465
$\kappa(A)$	15.268	ν	0.8080
$\ell(A)$	6.905	$\gamma_{ij(k)}$(A)	15.268
P	4	$\gamma_{ik(j)}$(A)	15.268
		χ(A)	6.905

The calculated effective interatomic potentials of ZnO are shown in Fig. 1. It appears that the presented TP potential give rise deep potential well than KTS and KTS-V2 potentials. This is shown that more long range character than others. The KTS-V3 potential exhibits the repulsive pair potential behavior.

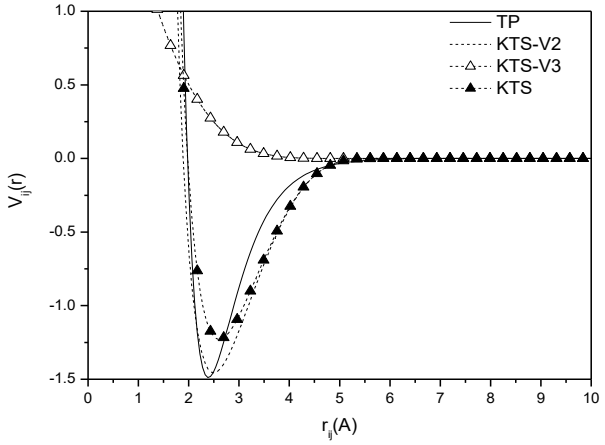

Fig.1. Pair interaction for ZnO using semi-empirical model potentials.

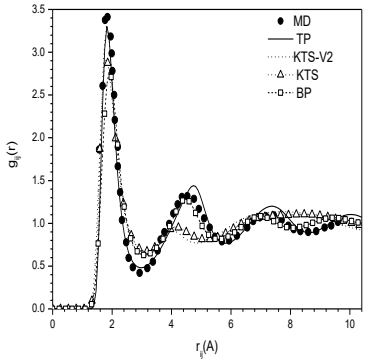

Fig. 2. Pair Distribution Function for ZnO at 2475K.

We compare the pair distribution functions calculated by TP, BP, KTS potentials with MD data [8]. There is a good agreement between TP and MD whereas the oscillations of $g_{ij}(r)$ calculated from TP is higher than MD after second and third coordination shell. The calculated $g_{ij}(r)$'s from KTS-V2 and KTS potentials reproduce same main peak position with MD, although the height of first peak are lower then that of MD. In the long range region, TP and BP potentials have almost the same peak position with MD except their height of peaks. KTS potentials are not good agreement with MD result and have damped oscillations. We can see those difficulties clearly for KTS potentials group.

In Fig. 3, we present our results of MSD obtained by TP, KTS and BP potentials for three representative temperatures: 2475K, 1000K and 500K. The MSD results for each potential are different. We notice that, time dependence of the mean square displacement shows typical behaviour for simple liquids at higher temperatures. For longer times, as soon as the motions become diffusive, the mean square displacement has a linear dependence on time. It is clear that the diffusion coefficients with KTS potential could be somewhat slower than others

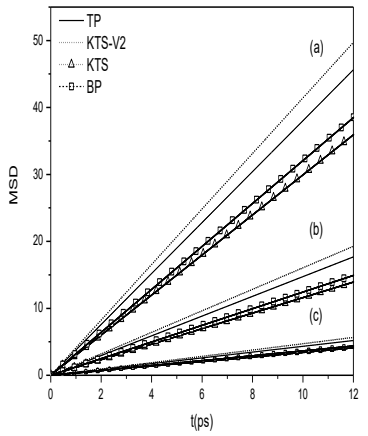

Fig. 3. Mean-Square Displacements for ZnO at (a) 2475K, (b) 1000K and (c) 500K.

In Fig 4, we present the normalized velocity autocorrelation functions obtained by TP, KTS and BP potentials for molten ZnO at 2475K. The results of KTS-V2 and BP show the backscattering minimum typical of high density systems at times around t=0.1ps followed by oscillations around zero.

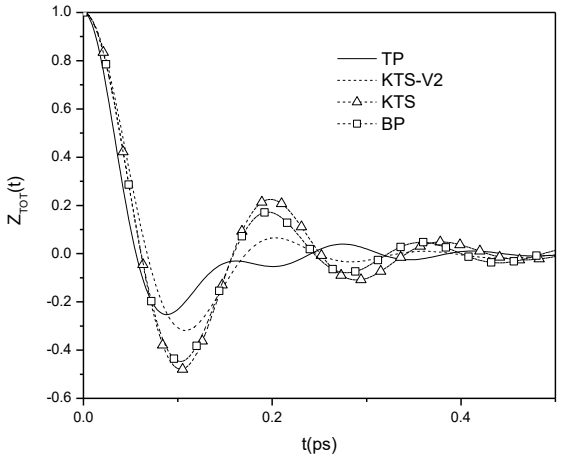

Fig. 4. Normalized velocity autocorrelation functions for ZnO calculated by TP, KTS and BP potentials at 2475K.

The normalized intermediate scattering functions obtained by the presented formalism are shown in Fig.5. It is observed that F(q,t) exhibits an oscillatory behavior for small q, which persists until around $q \approx 2q_p/3$. The q_p is the position of the main peak of the static structure factor which is about 2.314 A^{-1} for ZnO. The amplitude of oscillations of F(q,t) is stronger for the smaller q values and the oscillations take place around a globally decaying positive tail. For $q \leq 0.925A^{-1}$, F(q,t) has an oscillatory behavior for TP, whose period is 0.168ps and 0.159ps for $q=0.925A^{-1}$ and $q=1.54A^{-1}$ respectively. It is found that the smaller wave vectors shows the longer oscillatory period. For BP and KTS potentials F(q,t) has an oscillatory behavior at $q=0.925A^{-1}$ which periods are 0.198ps, 0.207ps respectively and for $q=1.54A^{-1}$ have periods at 0.204ps for BP and at 0.210ps for KTS potentials. At $q=2.31A^{-1}$, F(q,t) decreases monotonically with time for TP, KTS and BP. However, the half width at half maximum (HWHM) of F(q,t) is larger than those of other q values. The reason of this behavior is known it is at the main peak of S(q). At $q=3.471A^{-1}$, the decrease of F(q,t) is also monotonic though a shoulder are observed at $q=0.12A^{-1}$ for TP and $q=0.1A^{-1}$ for KTS-V2, KTS and BP.

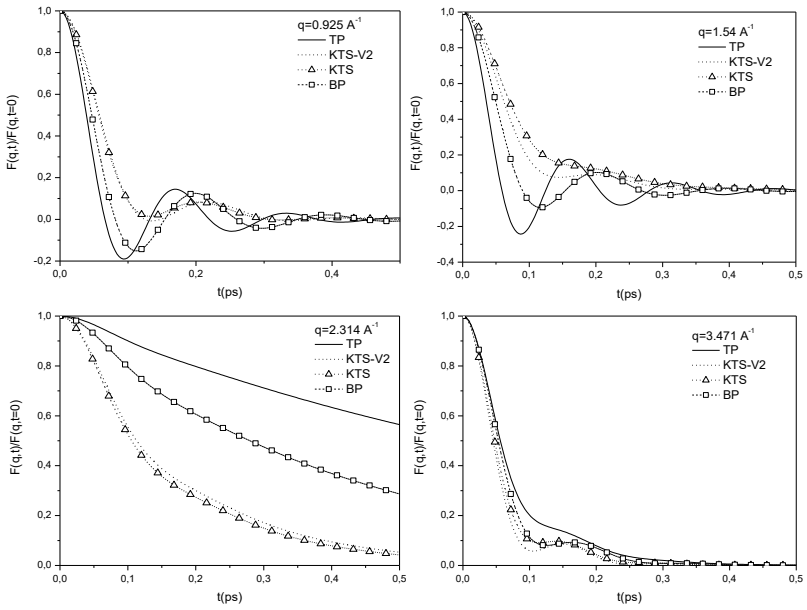

Fig. 5. The normalized intermediate scattering functions for ZnO at 2475K using TP, KTS and BP.

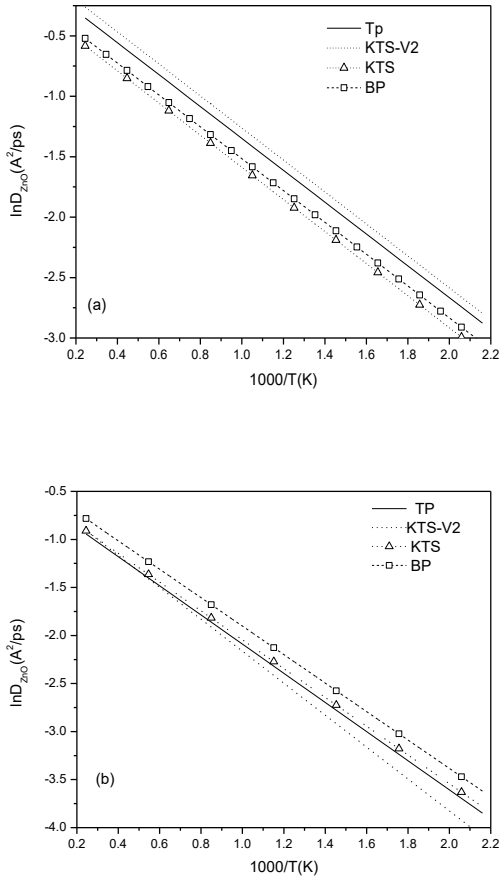

Fig. 6. Diffusion coefficients of ZnO plotted logarithmically as functions of inverse temperature (a) computed by Einstein (E) relation and (b)Green-Kubo (GK) relations.

It is clear in Fig. 6(a) that the diffusion coefficient *D* evaluated from the relation between the mean square displacement and time is well predicted. We can see that in Fig. 6(a), MSD values in Fig 3 are the same order with diffusion coefficients which found with Einstein relation. The value of *D* increases with increasing temperature. The temperature dependence of our diffusion coefficient data exhibits the Arrhenius-type behaviour. Fig 6(b) shows Green-Kubo diffusion coefficient results. There is different trends appeared in the calculated results of diffusion coefficients shown in Fig. 6. This may be related with the definition of the velocity autocorrelation functions. However experimental diffusion data are not available to compare our results.

3. Conclusions

The results of applicability of the presented semi-empirical three-body TP, KTS and rigid ion BP potentials for the properties of molten ZnO over wide range of temperatures are presented in this study. These calculations were performed for the functions not only fit to solid data but also liquid state properties. The VMHNC integral equation theory is carried out in structural calculations. We conclude that an empirical three body TP potential with the VMHNC method reproduces well the structural, atomic dynamics properties of molten ZnO than the presented other potentials. However we may note that there are no enough measurements and calculations for understanding the dynamics of molten ZnO. The theory used in our dynamic calculations was proposed for metallic systems. Thus it has been shown that the presented formalism for semi empirical potentials is

capable of providing a good description of molten ZnO. This method can be easily applied to the other metal oxides.

Acknowledgements

This work is supported from the Research Foundation of Trakya University under Project Number TUBAP 780.

References

[1] F. Z. Aoumeur, Kh. Benkabou, B. Belgoumene, Physica B **337** 292(2003).
[2] J. E Jaffe, A.C. Hess, Phys. Rev B **48** 7903 (1993)
[3] S. Desgreniers, Phys. Rev. B **58**, 14 102, 1998.
[4] G. Carlotti, D. Einstte, G. Sonian, D. Vamma, J. Phys. Condens. Matter **7**, 9147 1995.
[5] H. Karzel, W. Potzel, M. Kofferlein, W. Schiessl, M. Steiner, U.Hiller, G. M. Kalvius, D. W. Mitschell, T.P. Das, P. Blaha, K. Schwartz, and M. P. Pasternack, Phys. Rev. B **53**, 11 425, (1996).
[6] L. Gerward, J. S. Olsen, J. Synchrotron Radiat. 2 (1995) 233.
[7] J. E Jaffe, J. A. Snyder, Z. Lin, A.C. Hess, Phys. Rev B **62** 3, (2000).
[8] X. Sun, Q. Chen, C. Wang, Y. Li, J. Wang Physica **B355,** 126–133 (2005)
[9] X. Sun, Z. Liu, Q. Chen, Y. Chu, C. Wang, Physics Letters A **360** 362(2006)
[10] X. Sun, Z. Liu, Q. Chen, J. Yu, C. Wang, J. Phys. and Chem. of Solids **68** 249(2007)
[11] X.W. Sun, Z.J. Liu, Q.F. Chen, H.W. Lu, T. Song, C.W. Wang, Solid State Com.1**40** 219 (2006)
[12] X.W. Sun, Y.D. Chu, T. Song, Z.J. Liu, L. Zhang, X.G. Wang, Y.X. Liu, Q.F. Chen, (to be published in Solid State Commun. (2007)).
[13] A. Zaoui, W. Sekkal, Phys. Rev. B **66** 174106 (2002)
[14] J. Tersoff, Phys. Rev. B37, 6991 (1988).
[15] F.Z. Aoumeur-Benkabou, B. Belgoumène, Comp. Coup. of Phase Diagrams and Thermochemistry **28** 65-69 (2004).
[16] S. S. Dalgic, H. Gurbuz , M. Caliskan, O. Ozgec, J. Optoelectron. Adv. Mater. **7**,2059 (2005)
[17] S.S Dalgic, O. Ozgec (unpublished results)
[18] S.S Dalgic, O. Ozgec J. Optoelectron. Adv. Mater. **9**,1715 (2007)
[19] D. Kohen, J. C. Tully, F. H. Stillinger, Surf. Sci. **397**, 225 (1998).
[20] A.B. Belonoshko, Geochim. Cosmochim. Acta 58 (1994) 4039.
[21] G.J. Kramer, N.P. Farragher, B.W.H. van Beest, Phys. Rev. B 43 (1991) 5068.
[22] L. E. Gonzalez, D. J. Gonzalez, M. Silbert, Physica **B168**, 39 (1991); L. E. Gonzalez, D. J. Gonzalez and M. Silbert, Phys. Rev. **A45**, 3803 (1992);
[23] L.E. Gonzalez, D. J. Gonzalez, S. Dalgic, M. Silbert, Z. Phys. **B103,** 13 (1997).
[24] S. S. Dalgıc, S. Dalgıc, G. Tezgor, Phys. Chem. Liq. **40**, 539 (2002).
[25] L.E. Gonzalez, D.J. Gonzalez, M. Canales, Z. Phys.B100, 601 (1996)
[26] M.M.Alemany, J. Casas, C. Rey, L.E. Gonzalez, L.J. Gallego, Phys. Rev. **E56** (6), 6818 (1997)
[27] S. Dalgic,M. Colakogullari, S.S. Dalgic, J. Optoelectron. Adv. Mater **7** (4), 1993 (2005)
[28] F. Shimojo, K. Hoshino, M. Watabe, J. Phys. Soc. Japan **63**, 141 (1994)
[29] J.E. Jaffe, A.C. Hess Phys. Rev **B48**, 7903 (1993)

*Corresponding author: dserap@yahoo.com